
Article:

Fisher, A.J., Imran, M.N.B., Mann, C. orcid.org/0000-0002-8781-1652 et al. (4 more authors) (2020) Short communication : the dissolution of UK simulant vitrified high-level-waste in groundwater solutions. Journal of Nuclear Materials, 538. 152245. ISSN 0022-3115

https://doi.org/10.1016/j.jnucmat.2020.152245

Journal Pre-proof

Short communication: The dissolution of UK simulant vitrified high-level-waste in groundwater solutions

Adam J. Fisher, Mohammed N.B. Imran, Colleen Mann, Clémence Gausse, Russell J. Hand, Neil C. Hyatt, Claire L. Corkhill

PII: S0022-3115(19)31610-1

DOI: https://doi.org/10.1016/j.jnucmat.2020.152245

Reference: NUMA 152245

To appear in: *Journal of Nuclear Materials*

Received Date: 12 December 2019

Revised Date: 25 April 2020

Accepted Date: 14 May 2020

Please cite this article as: A.J. Fisher, M.N.B. Imran, C. Mann, Clé. Gausse, R.J. Hand, N.C. Hyatt, C.L. Corkhill, Short communication: The dissolution of UK simulant vitrified high-level-waste in groundwater solutions, *Journal of Nuclear Materials* (2020), doi: https://doi.org/10.1016/j.jnucmat.2020.152245.

Short communication: The dissolution of UK simulant vitrified high-level-waste in groundwater solutions

Adam J. Fisher, Mohammed N. B. Imran, Colleen Mann, Clémence Gausse, Russell J. Hand, Neil C. Hyatt and Claire L. Corkhill*

NucleUS Immobilisation Science Laboratory, Department of Materials Science and Engineering, University of Sheffield, Sheffield, S1 3JD, UK

* To whom correspondence should be addressed. Email c.corkhill@sheffield.ac.uk, phone +44 (0) 114 22 23632

Abstract

Dissolution of a simulant UK nuclear waste glass containing Mg, Ca and Zn was investigated over 35 d at 50 °C in water and simulant groundwater solutions. The dissolution rates were influenced subtly by the groundwater composition, following the trend, from least to most durable: clay > water > granite ≈ saline. Solutions were rapidly silica saturated but boron dissolution rates continued to increase. This is hypothesised to be due to the formation of secondary Mg-silicate precipitates, preventing the formation of a passivating silica gel layer and allowing glass dissolution to proceed at close to the maximum rate.

Key words: aluminoborosilicate glass, nuclear waste, chemical durability, corrosion, zinc, magnesium, calcium, groundwater.

Some reprocessed high-level-waste (HLW) in the United Kingdom will be immobilised in a Ca and Zn oxide modified Mixed Windscale (MW) base glass with a nominal composition of $4.2Li_2O{\cdot}8.6Na_2O{\cdot}6.0CaO{\cdot}6.0ZnO{\cdot}4.2Al_2O_3{\cdot}23.4B_2O_3{\cdot}47.6SiO_2$ wt.%, referred to as CaZn MW. The transition from regular MW to the CaZn MW base glass has been made to enhance the incorporation of high Mo-content Post-Operational-Clean-Out (POCO) waste from the decommissioning of the highly-active-storage tanks [1, 2]. At present, this glass is being used to immobilise reprocessing wastes only. Investigation of the short-term durability of the CaZn MW glass [3-5], compared with regular MW glass (both incorporating reprocessing waste), shows that the addition of CaO and ZnO improves durability in the short-term [3, 4]. However, there remains uncertainty with regard to the chemical durability of CaZn-glass, especially under conditions representative of geological disposal, including in groundwater and at expected temperatures. The presence of Mg, as both a glass component and a key constituent of groundwater, is known to trigger the formation of secondary phases, which accelerate glass corrosion [6-11]. Furthermore, similar effects have been observed for glasses incorporating even small quantities of Zn [5, 12].

This study aims to evaluate the influence of different simulant groundwater solution compositions, compared with pure water, on the dissolution rates of the CaZn MW28 glass (28 wt.% waste loading) in a short-term accelerated leaching experiment, and to identify the role of secondary phases in the dissolution mechanism.

CaZn MW28 was fabricated from a selection of oxide precursors and 28 wt.% of an inactive HLW calcine obtained from the National Nuclear Laboratory (NNL-UK) from the reprocessing of Oxide (o) and Magnox (m) spent nuclear fuel at a ratio of 75o:25m. The batch was melted at 1060 °C for 5 hours (including 4 hours stirring) and annealed at 500 °C for 1 hour. The measured composition, ascertained by Inductively Coupled Plasma-Optical Emission Spectroscopy (ICP-OES) analysis after total digest of the glass in hydrofluoric acid was (in wt.% (± 3 % uncertainty)): 3.2 Al_2O_3, 20.5 B_2O_3, 0.8 BaO, 4.9 CaO, 1.2 CeO_2, 0.4 Cr_2O_3, 1.4 Cs_2O, 1.8 Fe_2O_3, 3.3 Gd_2O_3, 0.1 HfO_2, 0.6 La_2O_3, 2.6 Li_2O, 1.5 MgO, 1.9 MoO_3, 6.9 Na_2O, 1.9 Nd_2O_3, 0.3 NiO, 0.6 Pr_2O_3, 0.3 RuO_2, 37.7 SiO_2, 0.4 Sm_2O_3, 0.3 SrO, 0.3 TeO_3, 0.2 Y_2O_3, 4.7 ZnO and 2.0 ZrO wt.%. The measured density obtained by helium pycnometry was 2.894 ± 0.003 g cm^{-3} (uncertainty calculated from the standard deviation of ten measurements).

Crushed glass particles (75 – 150 µm diameter) were prepared and Product-Consistency-Test-B (PCT-B) experiments, according to ASTM standard C1285-14 [13], were conducted at 50 °C in Ultra-High-Quality (UHQ) water (18.2 MΩ cm) (initial pH(RT) 7.2) and in three simulant groundwater solutions

(Table 1). The surface area to volume ratio was 2,000 m^{-1}, and duplicate experiments were performed for 1, 3, 7, 14, 28 and 35 days under oxic conditions. Synthetic groundwater solutions were prepared by addition of chemical reagents added to 1 L of distilled water [14], as shown in Table 1. A total of 1.08 g of glass and 10 mL of solution was used. The amount of glass dissolved was measured from the normalised mass of elements (*i*) (g m^{-2}) (NL_i), according to:

$$NL_i = (C_i - C_{i,b})/(f_i \times (SA/V)) \quad (1)$$

where C_i and $C_{i,b}$ are the average concentration of element, *i*, in the leachate and blank tests (solution only, no glass), respectively (mg L^{-1}), measured using ICP-OES (ThermoScientific iCAPDuo6300); f_i is the mass fraction of *i* in the glass (unitless) and *SA/V* is the surface area to volume ratio of the total particles (m^{-1}), based on the geometric surface area. Uncertainty in NL_i was calculated by the standard deviation of the sum of uncorrelated random errors (see supplementary data).

Two different approaches were used to assess the normalised dissolution rate of boron (NR_B, g m^{-2} d^{-1}). In the first case, the 1 – 35 d NL_B data were fitted using linear regression, and the uncertainty in NR_B was calculated from a chi-squared fit. In the second the data was fitted using:

$$NL_B = A\tan^{-1}(t/B) \quad (2)$$

where *A* and *B* are fitting constants and *t* is time; an inverse tan fit has previously been found to provide a good empirical fit to the normalised mass loss data for a number of glasses, including the International Simple Glass (ISG) [15, 16]. In this case an "initial" dissolution rate, often defined as the maximum rate of glass dissolution controlled by hydrolysis of the silicate network [17], was calculated by evaluating the slope at $t = 0$:

$$dNL_i/dt_{(t=0)} \quad (3)$$

The experiments performed here do not involve infinitely dilute conditions, therefore, the "forward" rate, where $Q = 0$, is not calculated (noting that *Q* refers to the ion activity product in Transition State Theory applied to glass corrosion [18 - 20]). Thus the rates calculated in Eqn (3) are the inferred rates at $t = 0$ and are termed "initial" rates for these experiments. After dissolution, dried particles (dried for 14h at 50 °C) were adhered to carbon tabs or mounted in epoxy and ground to

reveal a cross-section. Scanning Electron Microscopy (SEM) and Energy Dispersive Spectroscopy (EDS) were performed using a Hitachi TM3030 SEM (operating at an accelerating voltage of 15 kV) and a Bruker Quantax 70, respectively. X-ray diffraction (XRD) was performed on pristine and 35 d altered particles using a Bruker D2 Phaser X-ray diffractometer. An angular range of 10 < °2Θ < 70 with a 0.02° step size of 0.17° min^{-1} was used, with a total scan time of 110 minutes. The geochemical modelling package PHREEQ-C version 3 was used to calculate the saturation indices of various secondary phases in the leachates at all time points. The concentration of elements in the leachate and the leachate pH(RT) were used as input to calculate a range of possible phases saturated in solution according to the Lawrence Livermore National Laboratory (LLNL) database.

Table 1. Composition of three synthetic solutions representative of generic repository groundwaters (GW) [14].

Element	Concentration (mmol L^{-1})		
	Granitic GW [21]	Saline GW [21]	Clay GW [22]
Na	2.8	140	55
K	0.1	2.1	1.1
Ca	0.5	19.9	7.5
Mg	0.2	0.4	5.7
Cl	2.1	173	52.5
HCO_3	2.0	2.0	-
SO_4^{2-}	0.1	4.0	15
SiO_2	0.2	-	-
pH(RT)	8.2	7.7	6.5

The measured NL_B (commonly used as an indicator for glass corrosion since boron does not participate in alteration layer formation), showed that dissolution of CaZn MW28 glass followed the trend, from the least to the most durable after 35 d: clay > UHQ > granite ≈ saline (Fig. 1a). The dissolution rate of boron, NR_B, calculated using the two fitting methods described above are given in Table 2 and Fig. S1a. For all solutions except for the saline groundwater, the dissolution rate of boron calculated using the linear regression method between 1 and 35 d was approximately the same (within error) as that calculated at t = 0 using the inverse tan fit (Table 2). The similarity in the calculated rates suggests that for the granite, clay and UHQ solutions, the NR_B for the 35 d duration of the experiment was similar to the inferred initial rate (at t = 0), i.e. close to the maximum dissolution rate of the glass [12].

The NL_{Si} (Fig. 1b and S1b) increased rapidly before slowing; this is typically observed when glass undergoes the “rate drop” caused by the formation of a passivating silica gel layer before transition

into the residual rate (Stage II) of dissolution [23]. However, the NL_B data indicated that there was no rate drop. Considering that the glass dissolved at the "initial" rate (as at t = 0), this behaviour can be attributed to rapid saturation of the solutions with respect to silica, and the almost immediate precipitation of secondary silicate phases, thus preventing the formation of a passivating silica gel layer and allowing dissolution to proceed at a rapid rate. In previous studies, the drop in NL_{Si} was attributed to the formation of Mg-silicate phases [10, 11]. Indeed, there was a decrease in the NL_{Mg} for clay, UHQ and granite solutions. It seems reasonable to suggest that the formation of secondary Mg-silicate phases may, therefore, drive enhanced glass dissolution, at a relatively rapid rate (similar in magnitude to the "initial" rate, governed by silicate network hydrolysis), with the source of the Mg from both the solution and the glass (since this behaviour was also observed in UHQ where the only source of Mg was the glass).

In contrast, for the saline groundwater, the NR_B calculated using the linear regression method was considerably lower than the inverse tan fit, suggesting that the dissolution reaction of the glass in this solution was passivated by the formation of a silica gel layer, as typically observed in borosilicate glass dissolution. This was confirmed by the NL_{Si} data (Fig. 1b), which reached a residual rate at ~7 d. It is interesting to note that in this solution, the NL_{Mg} *increased*, rather than decreased. This is discussed further below.

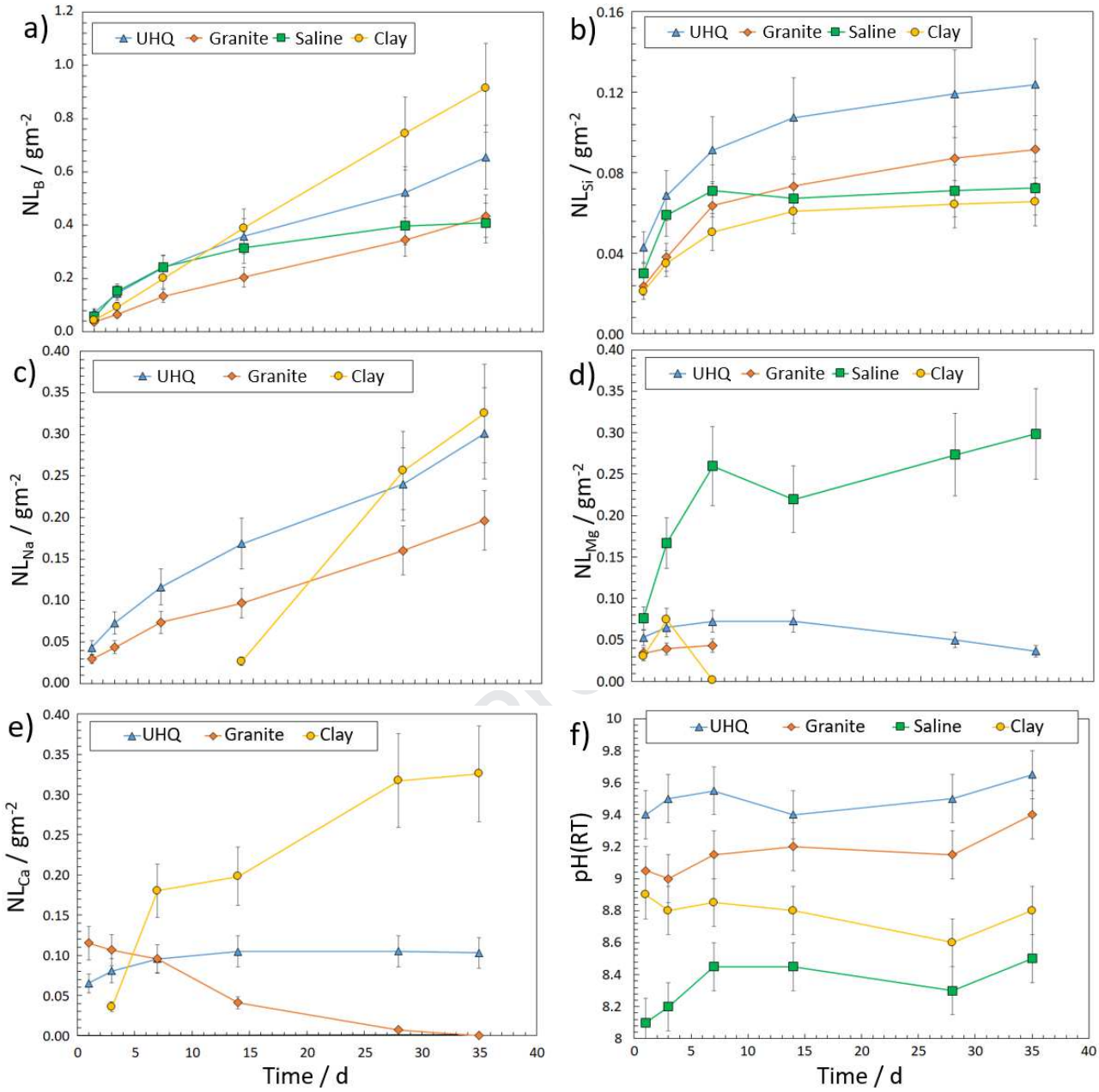

Fig. 1. (a – e) Normalized mass loss (NL) of elements, *i*, from CaZn MW28 particles during 35 d PCT-B leaching at 50°C in various groundwater compositions (errors bars are calculated from the sum of uncorrelated random errors); and f) pH(RT) measurements of the leachate. ($pH(RT)_{t=0}$: UHQ 7.2, granite 8.2, saline 7.7, clay 6.5).

Table 2. Normalised dissolution rate of boron (NR_B) calculated between 1 and 35 d for all experiments using a chi-square fit and between 14 and 35 d for the saline groundwater solution (since this was the linear part of the dissolution reaction) and the $NR_{B\ \&\ Si}$ "initial rate" as calculated at t=0 using an inverse tan fit.

Solution	B dissolution rate 1 - 35 d (NR_B / g m^{-2} d^{-1})	R^2	B initial rate (NR_B / g m^{-2} d^{-1})	R^2	Si initial rate (NR_{Si} / g m^{-2} d^{-1})	R^2
Clay	$(2.82 \pm 0.23) \times 10^{-2}$	0.999	$(2.8 \pm 0.7) \times 10^{-2}$	1.000	$(1.4 \pm 0.3) \times 10^{-2}$	0.975
UHQ	$(2.43 \pm 0.32) \times 10^{-2}$	0.882	$(2.0 \pm 0.5) \times 10^{-2}$	0.986	$(3.0 \pm 0.5) \times 10^{-2}$	0.975
Granite	$(1.54 \pm 0.12) \times 10^{-2}$	0.994	$(1.6 \pm 0.5) \times 10^{-2}$	0.988	$(1.5 \pm 0.2) \times 10^{-2}$	0.983
Saline	$(1.67 \pm 0.14) \times 10^{-2}$	0.421	$(4.8 \pm 0.5) \times 10^{-2}$	0.995	$(4.0 \pm 0.5) \times 10^{-2}$	0.989
Saline 14-35 d	$(0.46 \pm 0.42) \times 10^{-2}$	0.947	n/a	n/a	n/a	n/a

Analysis of the glass surface after dissolution by SEM / EDS (Fig. 2, Supplementary Figure 2) confirmed the enrichment of Mg (and Al) at the surface of the glass leached in clay groundwater, and a series of precipitates, approximately 2 – 5 µm in size, with a clay-like morphology, were first observed after 28 d of dissolution (Fig. 2b). X-ray diffraction (Fig. 3) analysis of glass dissolved for 35 d in each of the solutions did not reveal distinct crystalline phases (except for halite (NaCl), PDF 02-0818, in the saline groundwater), which is unsurprising given the low quantity of surface precipitates. Crystalline RuO_2 (PDF 21-1172) was observed in the pristine glass and in all glasses after 35 d of leaching; this is an expected feature of the waste glass being studied. It was not possible to observe a silica gel layer on the surface of the glass samples at the resolution employed, with the possible exception of the glass corroded in the saline solution which, after 35 d, appeared to show a "peeled" dehydrated gel layer with the glass surface underneath (Fig. S2d).

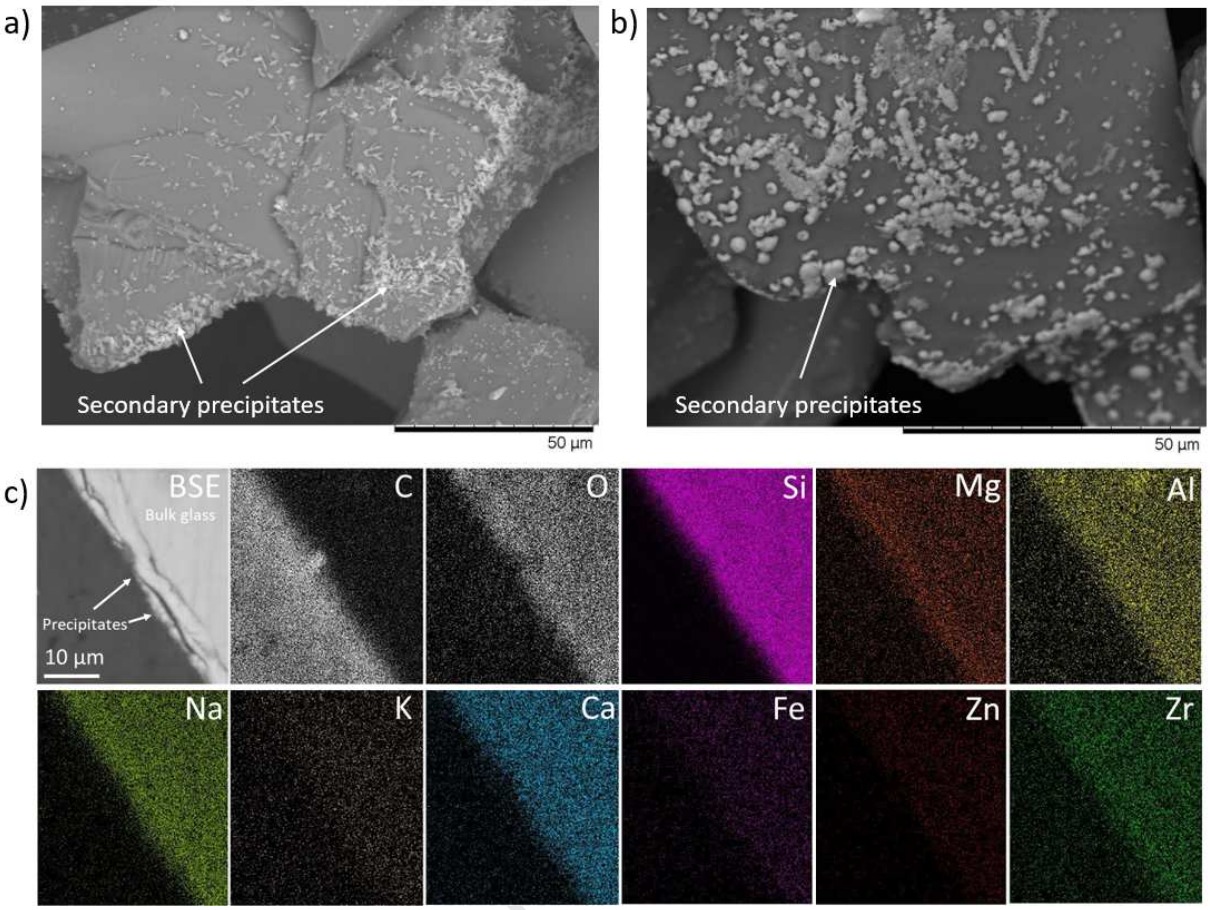

Fig. 2. BSE-SEM image and elemental mapping of CaZn MW28 after 35 d of leaching at 50 °C in clay groundwater.

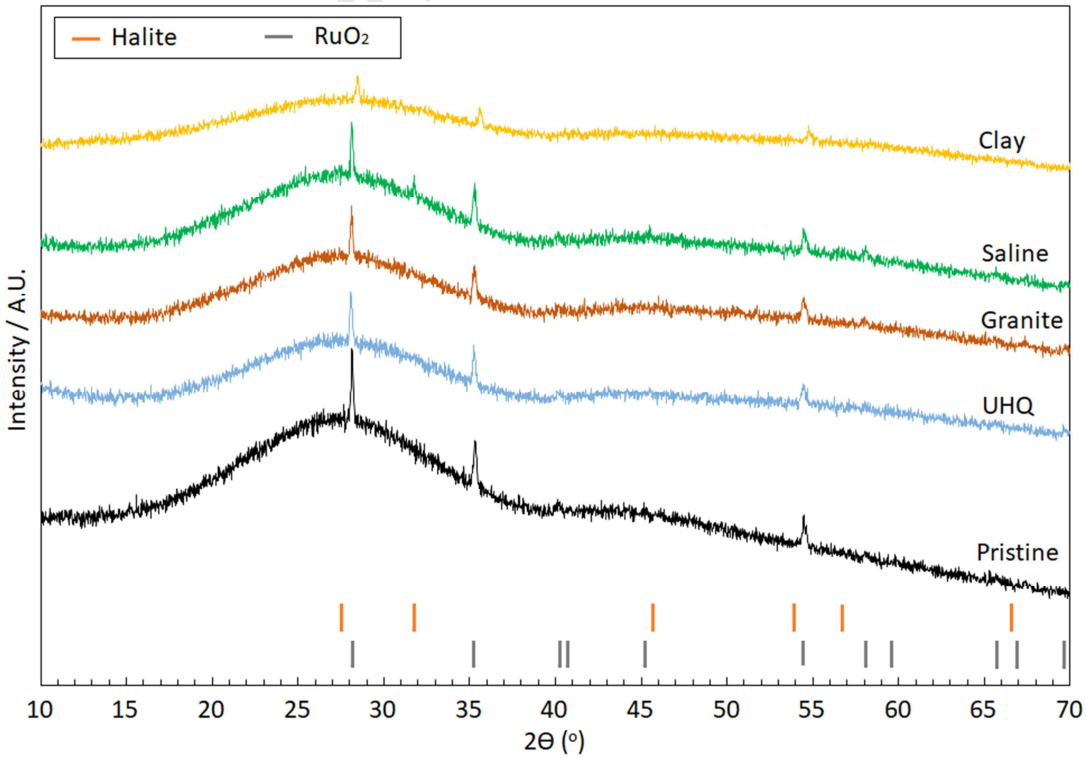

Fig. 3. XRD traces of CaZn MW28 particles pre- and post-35 d PCT-B leaching at 50 °C in UHQ and groundwater compositions.

Further indication that there was rapid onset of silica saturation in all solutions, and that Mg-silicate phases may have precipitated, is given by PHREEQ-C geochemical modelling of the solution leachates. Figure 4 shows that the solutions of all experiments were predicted to be saturated with respect to a number of phyllosilicate phases, rich in Mg, including saponite ($Mg_{3.165}Al_{.33}Si_{3.67}O_{10}(OH)_2$) and sepiolite ($Mg_4Si_6O_{15}(OH)_2{\cdot}6H_2O$). Additionally, they were saturated with respect to a range of Ca-bearing zeolites including mesolite ($Na_2Ca_2(Al_2Si_3O_{10})_3{\cdot}8H_2O$), scolecite ($CaAl_2Si_3O_{10}{\cdot}3H_2O$) and laumonite ($CaAl_2Si_4O_{12}{\cdot}4H_2O$)) at every time point, in accordance with the observed reduction in the NL_{Ca}, which was particularly evident for the granite and saline groundwaters.

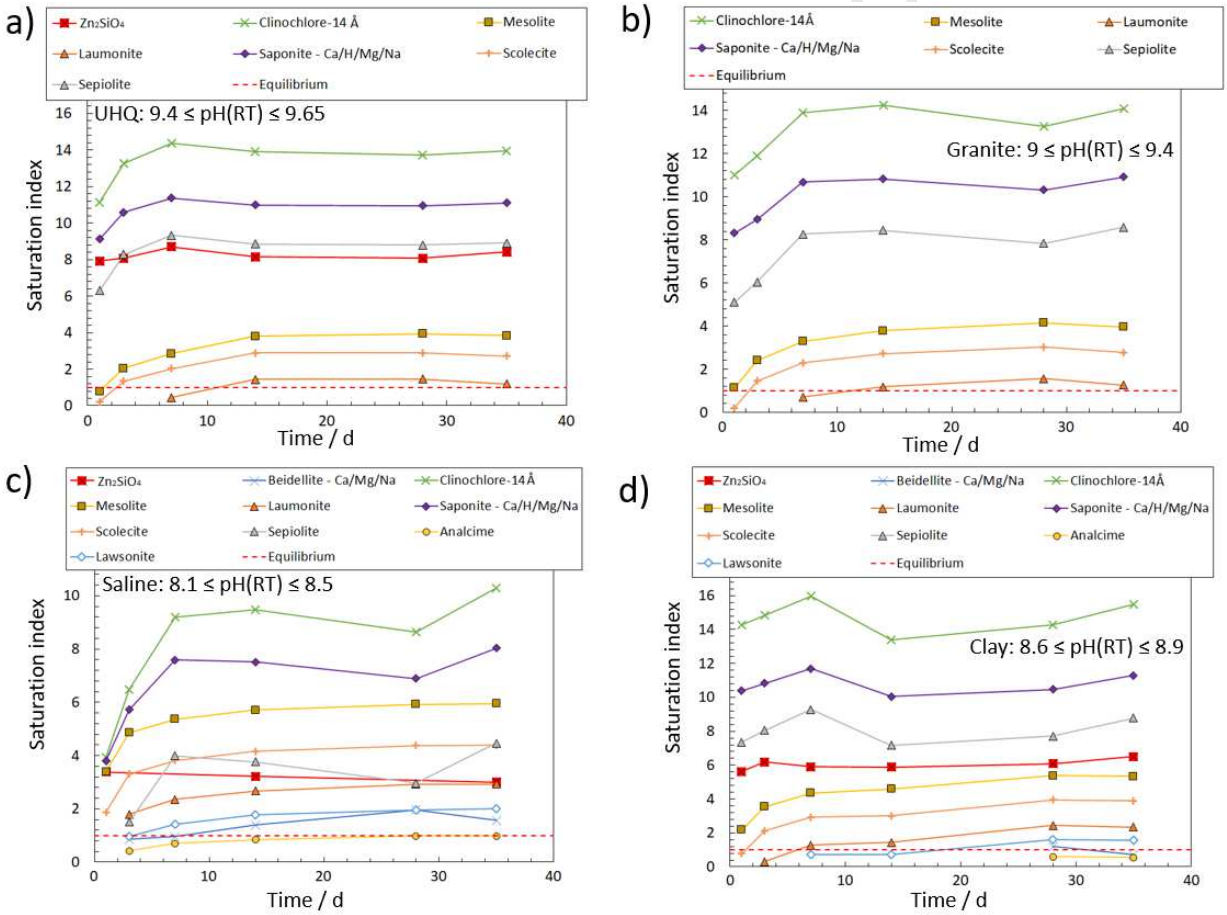

Fig. 4. PHREEQ-C geochemical modelling of the leachate from CaZn MW28 post 35 d PCT-B tests at 50 °C in (a) UHQ water; (b) granite; (c) saline and; (d) clay groundwater solutions. The measured input pH(RT) range of each data set is provided. Chemical formulae for each phase is provided in Table S1.

It is widely understood that Ca can be readily incorporated into silica gel layers, which has the effect of strengthening the gel layer and making it more resistant to dissolution in the short-term [11, 24–29]. The only experiment in which a silica gel layer was observed (and inferred from NL_i data) was that performed in the saline solution, which had an initial Ca concentration of 19.9 mmol L^{-1} (Table

1). Unlike the other groundwaters, the NL_{Ca} was negative in the saline solution; since NL_i values are calculated by subtracting the concentration of Ca in the blank solution (Eqn. 1), this indicates that there was significant removal of Ca from the solution, either into the silica gel layer (Fig. S2d) or secondary precipitates. Furthermore, in contrast to all of the other solutions, the NL_{Mg} in the saline solution appeared to increase rather than decrease (Fig. 1d), suggesting that Mg leached from the glass and remained in solution rather than participating in silica gel charge compensation or secondary precipitate formation. This is in agreement with Aréna *et al.* [26] who reported that Ca incorporation into the gel layer of the ISG dissolved in Mg-rich clay groundwater was favoured over Mg incorporation.

Interestingly, the clay groundwater contained significantly more Ca than the UHQ and granite solutions, yet the NL_{Ca} did not decrease, indicating that it was not removed from solution. This highlights the competition for Ca^{2+} and Mg^{2+} to form secondary silicate precipitates [16, 29–30], that favour Mg over Ca. This can be attributed to the more negative Gibbs Free Energy of hydration for Mg ($\Delta G_{Hyd}(Mg^{2+})$ -1830 kJ mol^{-1}, compared with ($\Delta G_{Hyd}(Ca^{2+})$ of -1505 kJ mol^{-1} for Ca) [31], which shows that Mg-silicates are thermodynamically more likely to form. Although Ca has a more favourable adsorption constant than Mg ($K_{ads} = 10^{-5.9}$ for Ca compared with $10^{-6.2}$ for Mg) and a higher ligand exchange rate ($K_{ex} = 10^{8.5}$ for Ca and $10^{5.2}$ for Mg), both of which favour the incorporation of Ca within the silica gel layer of corroding glass [29, 32], if Mg ions react with dissolving silica from the glass before a gel layer can form, there can be no Ca-silica gel layer.

The observation that the NL_{Mg} was significantly greater in the saline groundwater compared to all other solutions investigated may also be explained by the lower pH imposed by the saline system (Fig. 1f), inhibiting the formation of Mg-silicate phases [26]. This is consistent with the study by Thien *et al.* [8], who found that the precipitation of saponite ($Ca_{0.25}(Mg,Fe)_3((Si,Al)_4O_{10})(OH)_2 \cdot nH_2O$), was more efficient at pH 9, while at pH < 9, Mg was partially incorporated into the gel in a charge compensating role.

Previous studies have shown the propensity for the precipitation of Zn-silicate phases, such as hemimorphite ($Zn_2(SiO_4) \cdot H_2O$), upon the dissolution of Zn-containing MW glasses [33-34]. Furthermore, the hydrated zinc silicate phase, zincsilite ($Zn_3Si_4O_{10}(OH)_2 \cdot 4(H_2O)$), was proposed to form upon SON68 dissolution [35]. The Gibbs Free Energy of hydration of Zn^{2+} is more negative than that of Mg^{2+} ($\Delta G_{Hyd}(Zn^{2+})$ is -1955 kJ mol^{-1} and $\Delta G_{Hyd}(Mg^{2+})$ is -1830 kJ mol^{-1}), indicating that if Mg-silicates are capable of forming, then it is highly likely that Zn-silicates will also form, should Zn be

dissolved from the glass. In a simple ternary borosilicate glass composition containing Zn, it was hypothesised that the precipitation of Zn-silicate prevents the re-condensation of silica to form a gel layer, sustaining glass dissolution [12], which agrees well with the behaviour observed in the present study.

In the granite groundwater solution there was no Zn detected, suggesting that Zn was not released to solution (Fig. 5). In the UHQ, saline and clay groundwater solutions, however, it was possible to measure Zn in solution but the concentrations were close to the detection limit of the instrument (approx. 0.01 ppm) and, as such, had large errors associated with their values. Despite the absence of evidence for Zn-silicates in SEM/EDS and XRD analyses in this short duration study, geochemical modelling of all solutions showed that Zn_2SiO_4 was predicted to be stable. While it is highly unlikely that this phase would form under the hydrothermal conditions of the dissolution experiments performed here, it shows that Zn-silicate phases could be stable.

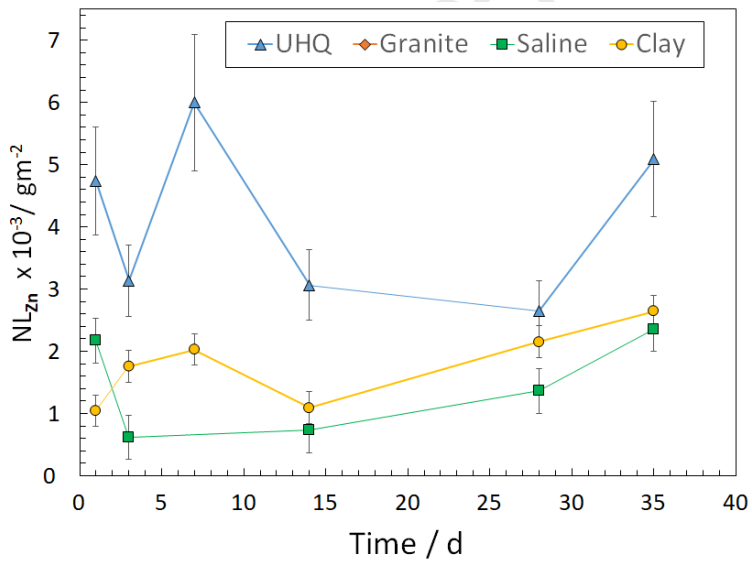

Fig. 5. Normalised mass loss of Zn (NL_{Zn}) from CaZn MW28 particles during 35 d PCT-B leaching at 50°C in various groundwater compositions calculated from elemental concentration values (ppm) at the limits of instrument detection.

This study highlights the fact that different groundwaters exert a subtle influence on the short-term dissolution rate of CaZn MW28 glass. Rapid onset of silica saturation and Mg-silicate precipitation [9], as predicted by geochemical modelling of the solutions and tentatively identified by SEM/EDS, is the postulated reason for elevated dissolution rates, where Mg from both the glass and the solution likely prevents the re-condensation of silica to form a gel layer, sustaining glass dissolution at a rate similar in magnitude to the "initial" rate. The same solubility limiting phases were predicted to form in all solutions (Fig. 4), therefore, the differences in dissolution rate may be attributed to the kinetics of formation and the quantity of the elements in each solution. The exception is saline groundwater,

which may have promoted the formation of a passivating silica gel layer (Fig. S2d), did not show a propensity for Mg-silicate formation and had amongst the lowest dissolution rates.

The dissolution behaviour observed here is not well described by any of the accepted dissolution rate definitions: the initial rate is widely defined as the congruent, linear release of elements at the maximum rate controlled by hydrolysis of the silica network [17]; the residual rate occurs once the solution is saturated with respect to silica and glass dissolution is no longer driven by silicate hydrolysis but by diffusion processes (of ions through the silica gel layer) [17], while the massive precipitation of secondary silicates (almost exclusively zeolite phases) and rapid dissolution of the glass is known as “rate resumption”, which is typically associated with a significant pH increase [36]. In contrast, in the groundwater solutions of the present study, the CaZn MW28 glass apparently underwent “initial” rate dissolution while under conditions of silica saturation, promoted by aggressive precipitation of secondary Mg-phyllosilicate phases, with no change in pH. Seemingly all of the currently defined stages of dissolution occurred simultaneously, thus an alternative definition for such behaviour is required.

As radioactive waste geological disposal programmes mature, and dissolution rates are determined in increasingly complex groundwater solutions, this study serves to highlight the need for further investigation of systems containing divalent cations and their influence on glass dissolution behaviour. This is also important for new glass compositions developed to progress the decommissioning of nuclear facilities, such as the incorporation of Zn in POCO glass compositions. In particular, further detailed studies of the role of Mg and Zn-silicate precipitation in glass dissolution, in conjunction with appropriate thermodynamic databases, are required to understand whether Zn-silicate influences glass dissolution by the same mechanism, and to the same magnitude, as Mg-silicate precipitation, and to determine if there is an additive [37] or competitive effect when both Mg and Zn are present.

Acknowledgements

This work was funded, in part, by the EPSRC Next Generation Nuclear Centre for Doctoral Training Centre under grant EP/L015390/1. Financial support for CLC from the EPSRC (ECR Fellowship; EP/N017374/1) is acknowledged. This research was performed at the MIDAS Facility, at the University of Sheffield, which was established with support from the UK Department of Energy and Climate Change. Thanks are given to Dr. Mike Harrison from the National Nuclear Laboratory (UK)

for the supply of the waste calcine and we thank an anonymous reviewer and Professor Stéphane Gin for helpful discussions with regards to defining dissolution rate regimes.

Data availability

The raw data required to reproduce these findings are available upon request.

References

[1] B. F. Dunnett, N. R. Gribble, R. Short, E. Turner, C. J. Steele and A. D. Riely, Vitrification of high molybdenum waste, *Glass Technol-Part A.* **53** (4) (2012) 166-171.

[2] R. Short, N. R. Gribble, A. D. Riley, Widening the envelope of UK HLW vitrification-experimental studies with high level waste loadings and new product formulations on a full scale non-active vitrification plant, Waste Management Conference, Phoenix, AZ, 24-28th February, 2008.

[3] Matlack et al. *Sci. Bas. Nuc. Was. Man. XXII*, Paper 9.55, Mater. Res. Soc. Fall Meeting (1998).

[4] M. T. Harrison and G. C. Brown, Chemical durability of UK vitrified high level waste in Si-saturated solutions, *Mat. Let.* **221** (2018) 154-156.

[5] A. J. Fisher, M. T. Harrison, N. C. Hyatt, R.J Hand and C. L. Corkhill, The dissolution of simulant UK Ca/Zn-modified nuclear waste glass: Insight into Stage III behaviour, *MRS. Adv*. *Scientific Basis for Nuclear Waste Management XLIII. MRS Advances.* Cambridge University Press. **5**, [3-4] (2020) 103-109.

[6] E. Curti, J. L. Crovisier, G. Morvan and A. M. Korpoff, Glass dissolution parameters: update for Entsorgungsnachweis, Nagra Technical Report NTB 02-21, Nagra, Wettingen, Switzerland (2003).

[7] E. Curti, J. L. Crovisier, G. Morvan and A. M. Karpoff, Long-term corrosion of two nuclear waste reference glasses (MW and SON68) : A kinetic and mineral alteration study, *Appl. Geochem.* **21** (2006) 1152-1168.

[8] B.M.J. Thien, N. Godon, A. Ballestero, S. Gin and A. Ayral, The dual effect of magnesium on the long-term alteration rate of AVM nuclear waste glasses, *J. Nucl. Mater.* **427** (2012) 297-310.

[9] B. Fleury, N. Godon, A. Ayral and S. Gin, SON68 glass dissolution driven by magnesium silicate precipitation, *J. Nucl. Mater.* **442** (2013) 17-28.

[10] T. Maeda, H. Ohmori, S. Mitsui and T. Banba, Corrosion behaviour of simulated HLW glass in the presence of magnesium ion, *Int. J. Corr*. 796457 (2011).

[11] P. Jollivet, P. Frugier, G. Parisot, J.P. Mestre, E. Bracky, S. Gin and S. Schumacher, Effect of clayey groundwater on the dissolution rate of the simulated nuclear waste glass SON68, *J. Nucl. Mater*. **420** (2012) 508-518.

[12] S. Gin, P. Frugier, P. Jollivet, F. Bruguier and E. Curti, New insight into the residual rate of borosilicate glasses: effect of S/V and glass composition, *Int. J. Appl. Glass. Sci.* **4** [4] (2013) 371-382.

[13] ASTM - Standard Test Methods for Determining Chemical Durability of Nuclear, Hazardous and Mixed Waste Glasses and Multiphase Glass Ceramics: The Product Consistency Test (PCT) (ASTM C1285-14). 1–26 (2014). doi:10.1520/C1285-14.2

[14] R.G.W. Vasconcelos, A. Idiart, N. C. Hyatt, J. L. Provis and C. L. Corkhill, Leaching of Nirex Reference Vault Backfill cement by clay, granite and saline groundwaters. In: *MRS Advances. Scientific Basis for Nuclear Waste Management XLI*. Cambridge University Press (2018) 1175-1180.

[15] D. J. Backhouse, C.L Corkhill, N.C Hyatt and R.J. Hand, Investigation of the role of Mg and Ca in the structure and durability of aluminoborosilicate glass, *J. Non-Cryst. Solids,* **512** (2019) 41-52.

[16] D. J. Backhouse, A. J. Fisher, J. J. Neeway, C.L. Corkhill, N.C. Hyatt and R.J. Hand, Corrosion of the International Simple Glass under acidic to hyperalkaline conditions, *npj Mater. Degrad.* 2:29 (2018). Doi.org/10.1038/s41529-018-0050-5

[17] S. Gin, X. Beaudoux, F. Angeli, C. Jégou and N. Godon, Effect of composition on the short-term and long-term dissolution rates of ten borosilicate glasses of increasing complexity from 3 to 30 oxides. *J. Non-Cryst. Solids*, 358 (2012), 2559-2570.

[18] Eyring H. The activated complex in chemical reactions. *J. Chem. Phy*. **3** (1935) 107-114.

[19] Grambow B. A general rate equation for nuclear waste glass corrosion. *Mater. Res. Soc. Symp. Proc.* 44 (1985) 15-27.

[20] Strachan D. Glass dissolution as a function of pH and its implications for understanding mechanisms and future experiments. *Geochim. Cosmochim. Acta.* **219**, (2017) 111-123.

[21] M. Gascoyne, Influence of grout and cement on groundwater composition. POSIVA Working Report 2002-07, Posiva Oy (2002).

[22] A. Vinsot, S. Mettler, and S. Wechner, In situ characterization of the Callovo-Oxfordian pore water composition. *Phys. Chem. Earth*, **33** [1] (2008) 75-86.

[23] J. D. Vienna, J. V. Ryan, S. Gin and Y. Inagaki, Current understanding and remaining challenges in modelling long-term degradation of borosilicate nuclear waste glasses, *Int. J. Appl. Glass. Sci.* **4** [4] (2013) 283-394.

[24] J. M. Schofield, S. W. Swanton, B. Farahani, B. J. Myatt, T. G. Heath and S. E. Burrows, Experimental studies of the chemical durability of UK HLW and ILW glasses, Amec report to Radioactive Waste Management (UK), RWM005105, AMEC/103498/04 Issue 1 (2017).

[25] C. A. Utton, R. J. Hand, P. A. Bingham, N. C. Hyatt, S. W. Swanton and S. J. Williams, Dissolution of vitrified wastes in a high-pH calcium-rich solution, *J. Nucl. Mater.* **435** (2013) 112-122.

[26] H. Aréna. D. Rébiscoul, R. Podor, E. Garcès, M. Cabie, J. –P. Mestre and N. Godon, Impact of Fe, Mg and Ca elements on glass alteration: Interconnected processes, *Geochim. Cosmochim. Ac.* **239** (2018) 420- 445.

[27] C. L. Corkhill, N. J. Cassingham, P. G. Heath and N. C. Hyatt, Dissolution of UK high-level-waste under simulated hyperalkaline conditions of a collocated geological disposal facility, *Int. J. App. Gla. Sci*. **4** [4] (2013) 341-356.

[28] T. Chave, P. Frugier, S. Gin and A. Ayral, Glass-water interphase reactivity with calcium rich solution, *Geochim. Cosmochim. Ac.* **75** (2011) 4125-4139.

[29] C. Mann, A study of the dissolution of UK nuclear waste glass in cement waters, Ph.D Thesis, The University of Sheffield (2019).

[30] B. Lothenbach, D. Nied, E. L'Hôpital, G. Achiedo and A. Dauzères, Magnesium and calcium silicate hydrates, *Cement Concrete Res,* **77** (2015) 60–68.

[31] Y. Marcus, Thermodynamics of solvation of ions, *J. Chem. Soc. Faraday Trans*, **87** (1991) 2995-2999.

[32] M. Collin and M. Fournier, Impact of alkali on the passivation of silicate glass. *npj Mater. Degrad.* 1–10 (2018). doi:10.1038/s41529-018-0036-3

[33] H. Zhang, C. L. Corkhill, P. G. Heath, R. J. Hand, M. C. Stennett, N. C. Hyatt. Effect of Zn- and Ca-oxides on the structure and chemical durability of simulant alkali borosilicate glasses for immobilisation of UK high level wastes, *J. Nucl. Mater.* **462** (2015) 321-328.

[34] N. J. Cassingham, C. L. Corkhill, M. C. Stennett, R. J. Hand and N. C. Hyatt, Alteration layer formation of Ca- and Zn-oxide bearing alkali borosilicate glasses for immobilisation of UK high level waste: A vapour hydration study, *J. Nucl. Mater.* **479** (2016) 639-646.

[35] M. Debure, Y. Linard, C. Martin and F. Claret, In situ nuclear-glass corrosion under geological repository conditions, *npj Mater. Degrad.* 3:38 (2019). Doi.org/10.1038/s41529-019-0100-7

[36] M. Fournier, S. Gin and P. Frugier, Resumption of nuclear glass alteration: State of the art. *J. Nucl. Mater.* **448** (2014) 348-363.

[37] H. Aréna, N. Godon, D. Rébiscoul, R. Podor, E. Garcès, M. Cabie, J. –P. Mestre. Impact of Zn, Mg, Ni and Co elements on glass alteration: Additive effects. *J. Nucl. Mater.* **470** (2016) 55-67.

Appendix. Supplementary data

Uncertainty in NL_i was calculated by the standard deviation of the sum of uncorrelated random errors [16] according to:

$$\sigma_f = \sqrt{\sum_{i=1}^{n} \left(\frac{\partial f}{\partial x_i}\right)^2 \sigma_i^2} \qquad [S1]$$

where σ_f is the standard deviation of $f(x_i)$, where x_i is the parameter pertaining to element *i* and σ_i is the standard deviation of parameter x_i. Substituting Equation 1 (main text) into Equation S1, and using a relative error, $\widehat{\sigma}_{NL_i} = \frac{\sigma_{NLi}}{NL_i}$ gives:

$$\widehat{\sigma}_{NL_i} = \sqrt{\frac{\left(\widehat{\sigma}_{C_{i,S}} C_{i,S}\right)^2 + \left(\widehat{\sigma}_{C_{i,b}} C_{i,0}\right)^2}{\left(C_{i,S} - C_{i,0}\right)^2} + \widehat{\sigma}_{f_i}^2 + \widehat{\sigma}_{SA/V}^2} \qquad [S2]$$

from which the experimental uncertainty on r_i can be derived. Relative errors of 10%, 10%, 3% and 15% were ascribed to C_i, $C_{i,o}$, f_i and SA/V respectively.

a)

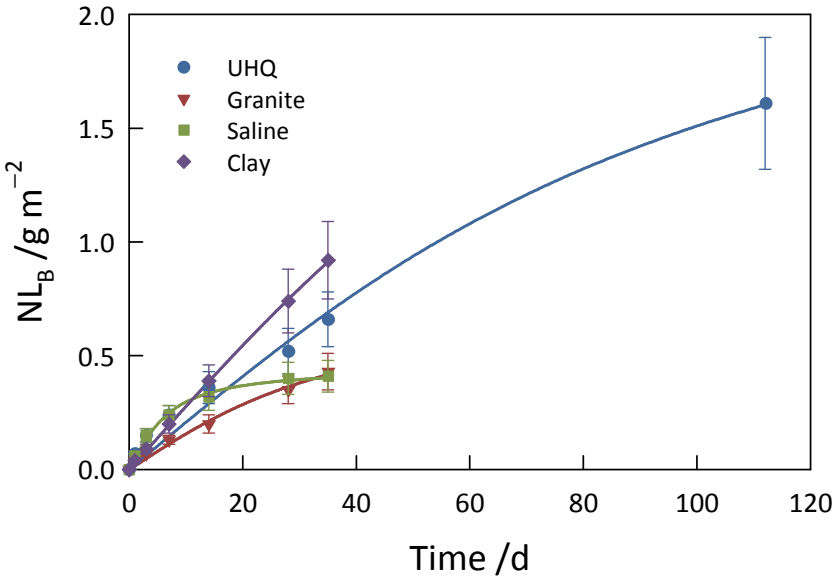

b)

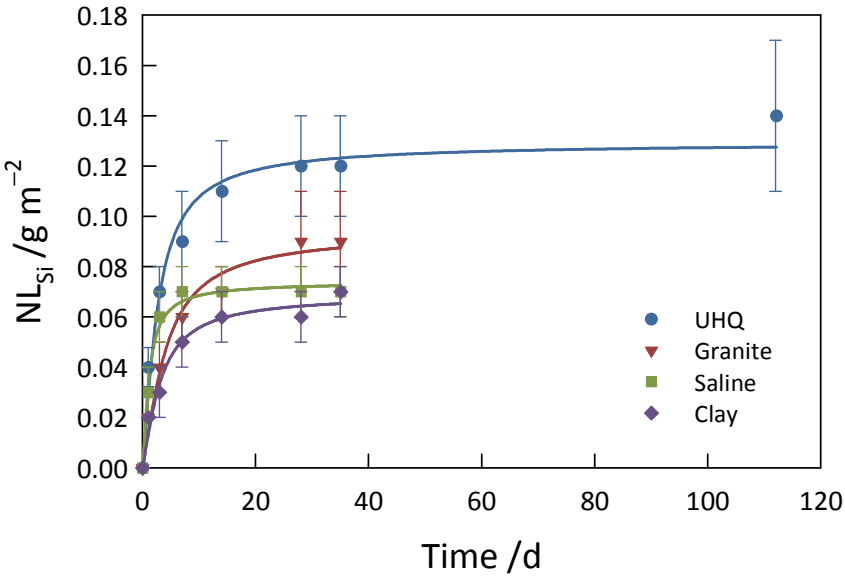

Figure S1. (a) Inverse tan empirical fit to the normalised mass loss (B & Si) data; and (b) PCT-B tests for CaZn MW28 at 50°C, SA/V = 2,000 m^{-1}, in various groundwater solutions and UHQ water. Note the additional data point at 112 d for the UHQ test only. Uncertainty in NL_i was calculated by the standard deviation of the sum of uncorrelated random errors (Eqns. 1, S1 & S2).

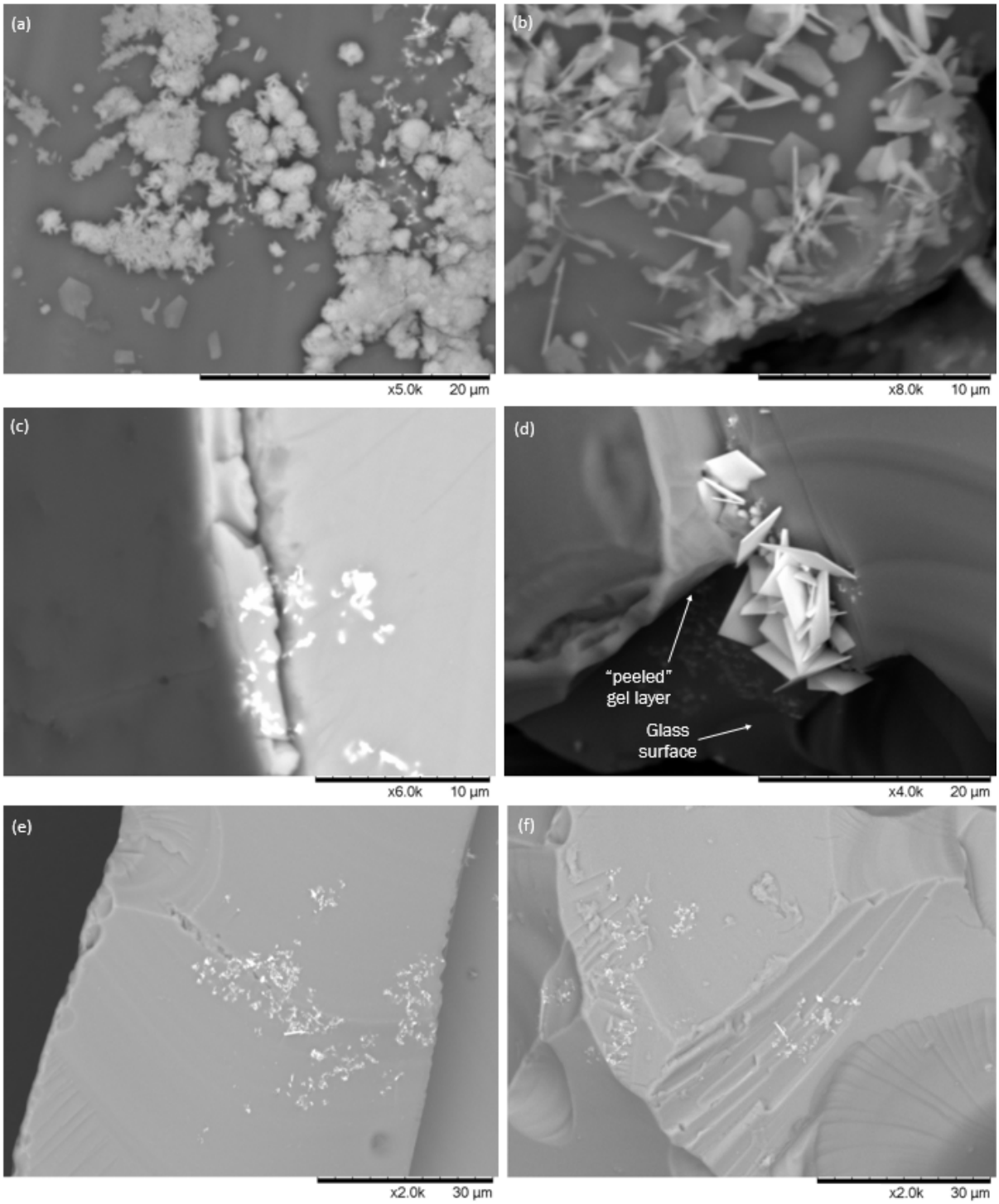

Figure S2. BSE-SEM images of the CaZn MW28 glass surface after 35 d of dissolution in groundwater at 50°C showing (a) and (b) the range of crystalline phases precipitated on the surface of glass dissolved in clay groundwater; (c) the absence of a distinct gel layer at the surface of the glass dissolved in clay groundwater (cross section image); (d) possible evidence for a dehydrated silica gel layer peeled back from the glass surface, in addition to halite crystallites for glass dissolved in saline groundwater; (e) glass surface from the UHQ water and (f) granite tests, which did not show any surface precipitation or gel layers (the bright phases are crystallite of RuO_2).

Table S1. Chemical formulae for all predicted phases from PHREEQ-C geochemical modelling

Mineral phase	Chemical formula
Analcime	$NaAlSi_2O_6 \cdot H_2O$
Beidellite - (Ca,Mg)	$(Ca,Mg)_{0.165}Al_{2.33}Si_{3.67}O_{10}(OH)_2$
Beidellite - Na	$Na_{0.61}Al_{4.7}Si_{7.32}O_{20}(OH)_4$
Clinochlore - 14 Å	$Mg_5Al_2Si_3O_{10}(OH)_8$
Laumonite	$CaAl_2Si_4O_{12} \cdot 4H_2O$
Lawsonite	$CaAl_2Si_2O_7(OH)_2 \cdot H_2O$
Mesolite	$Na_{0.676}Ca_{0.657}Al_{1.99}Si_{3.01}O_{10} \cdot 2.647H_2O$
Saponite – Ca	$Ca_{0.165}Mg_3Al_{0.33}Si_{3.67}O_{10}(OH)_2$
Saponite – H	$H_{0.33}Mg_3Al_{0.33}Si_{3.67}O_{10}(OH)_2$
Saponite – Mg	$Mg_{3.165}Al_{0.33}Si_{3.67}O_{10}(OH)_2$
Saponite – Na	$Na_{0.33}Mg_3Al_{0.33}Si_{3.67}O_{10}(OH)_2$
Scolecite	$CaAl_2Si_3O_{10} \cdot 3H_2O$
Sepiolite	$Mg_4Si_6O_{15}(OH)_2 \cdot 6H_2O$
Zinc silicate	Zn_2SiO_4

Short communication: The dissolution of UK simulant vitrified high-level-waste in groundwater solutions

Adam J. Fisher, Mohammed N. B. Imran, Colleen Mann, Clémence Gausse, Russell J. Hand, Neil C. Hyatt and Claire L. Corkhill*

NucleUS Immobilisation Science Laboratory, Department of Materials Science and Engineering, University of Sheffield, Sheffield, S1 3JD, UK

Declaration of interests

☒ The authors declare that they have no known competing financial interests or personal relationships that could have appeared to influence the work reported in this paper.

☐The authors declare the following financial interests/personal relationships which may be considered as potential competing interests: